Chaos and bifurcations in ion traps of cylindrical and spherical design

R. Blümel, E. Bonneville, and A. Carmichael*
Fakultät für Physik, Albert-Ludwigs-Universität, Hermann-Herder-Strasse 3, D-79104 Freiburg, Germany
(Received 21 July 1997)

With the help of analytical and numerical methods we analyze the nonlinear dynamics of a single ion stored in periodically driven dynamical traps of cylindrical and spherical design. Sinusoidal and impulsive drives are investigated. Both traps exhibit a mixed phase space for both drives. Additionally there is a route to chaos via period-doubling bifurcations of the fundamental stable trapping island. We demonstrate that the bifurcation scenarios of the kicked and cw-driven traps are quantitatively close and qualitatively identical. [S1063-651X(98)01202-1]

PACS number(s): 05.45.+b, 32.80.Pj

I. INTRODUCTION

Over the past decades the static Kingdon trap [1,2], the Penning trap [3,4], and the Paul trap [5,6] have evolved into indispensible tools in many laboratories working on research topics ranging from the precision determination of fundamental natural constants [7] to the investigation of nonlinear phenomena [8,9], the construction of frequency standards [10], and quantum computers [11]. Other types of traps have already been proposed and used in actual experiments [12,13]. All these traps make use of strong focusing [14] to achieve charged-particle trapping. Recently, a different trap design was proposed that makes use of strong *defocusing* coupled with electrostatic attraction in order to achieve trapping [15–17]. The trap consists of two concentric metallic cylinders with a superposition of an ac and a dc voltage applied between them (see, e.g., Fig. 8 of Ref. [17]). Because of its resemblance to the static Kingdon trap, the cylindrical trap was named ''dynamic Kingdon trap.''

It was proved analytically that on the basis of this principle stable trapping is possible in both cylindrical and spherical geometries [15–17]. It was demonstrated that in analogy to the Paul and Penning traps the dynamic Kingdon trap is an ideal device for the investigation of storage, crystallization, and melting of large Coulomb clusters [16]. In fact, the existence of a deterministic route to single-ion chaos strongly suggests the possibility of deterministic melting of large Coulomb clusters stored in a dynamic Kingdon trap.

Following publication of the theoretical investigation of the dynamical Kingdon trap, we learned recently [18] that the dynamic Kingdon trap had already been proposed some 30 years ago by E. Teloy at the University of Freiburg. It was subsequently investigated under his direction by Bahr [19] in 1969 and Behre [20] in 1972. In the course of this early research a dynamic Kingdon trap was actually built in the laboratory and its storage properties were investigated [19,20]. In addition, the storage properties of the dynamic Kingdon trap were investigated by detailed computer simulations. Thus the early theory and experiments by Teloy, Bahr, and Behre demonstrated that the dynamic Kingdon trap is a working design for the storage of charged particles. The focus of these early investigations was on demonstrating the working principle of the trap and using the trap as a mass selective ion source. Thus the emphasis was on the simultaneous storage of dense clouds of many ions. Single-ion experiments were not realistically possible then since it requires a cooling mechanism and the most convenient cooling method, laser cooling, was not proposed until several years later [21].

Recently, the spherical trap proposed in [15,17] was the subject of experiments performed at the Max-Planck-Institute for Quantum Optics in Munich. These experiments succeeded in demonstrating stable confinement of charged microspheres in a trap of essentially spherical design [22], thus proving experimentally that the spherical traps proposed in [17] are a working design. Since, for concentric shells, the field in the trap is the same as the one generated by a suitable charge at the center of the trap, the spherical trap was called the ''monopole trap'' [22]. Storage times of the order of hours were recorded for single charged microspheres in the monopole trap. In addition, a first period-doubling bifurcation was observed to occur in the monopole trap.

Both types of traps, the ones based on strong focusing and the ones based on strong defocusing, operate according to the same general principle: A charged particle in an inhomogeneous rapidly oscillating electric field experiences a force pointing towards the direction of lower field strength. In other words, a charged particle in a rapidly oscillating electric field is a ''low-field seeker'' [6]. On the basis of this fact, the working principle of the dynamic Kingdon trap is immediately clear. No matter what the polarity of the particle, since the electric field diminishes towards the outer cylinder of the trap, the ac voltage drives the particle into the direction of the outer metallic electrode of the trap. This is a manifestation of the strong defocusing mechanism [15]. Counteracting the defocusing mechanism is the dc voltage. Its polarity is chosen such that it drives the charged particle back towards the inner cylinder. Since the dc focusing force and the ac defocusing force have different radial dependences [15,16], a judicious choice of dc and ac voltages produces a potential minimum in the free space between the two cylinders. If a cooling mechanism is provided, e.g., in the form of laser cooling [23,24], the charged particle may settle

*On leave from the Department of Physics, University of Sussex, Falmer, Brighton, United Kingdom.

down into this potential minimum and can be stored there, in principle, forever.

In this paper we focus on the nonlinear dynamics of a single ion stored in the dynamic Kingdon trap and the monopole trap. We show that the equations of motion of both types of traps are members of a class of nonlinear Mathieu equations. In contrast to the ideal versions of the ''classic'' traps, the static Kingdon trap, the Paul trap, and the Penning trap, a single ion stored in a dynamic Kingdon trap or a monopole trap may be chaotic. There are two types of chaos present in the dynamics of strong defocussing traps. (i) Both types of traps exhibit Hamiltonian chaos in certain regions of their phase space. (ii) A chaotic regime is also reached via a cascade of period-doubling bifurcations. In order to get a better qualitative insight into the mechanism of the period doublings and especially in order to get an analytical estimate for the onset of the bifurcations, we investigate here kicked versions of the cylindrical and spherical traps. It is shown that as far as the qualitative behavior of the bifurcation trees is concerned, the kicked versions and the continuously driven versions of the traps display the same behavior. Even quantitatively the bifurcation points of the kicked and the continuously driven traps are very close.

II. THE GENERALIZED MATHIEU EQUATION

In this section we show that the equations of motion of an ion in a dynamic Kingdon trap, or a monopole trap, are special cases of the *generalized Mathieu equation*

$$\ddot{x}+[s-2\eta f(2t)]x^{\alpha}=0. \tag{2.1}$$

This class of second-order differential equations is characterized by three control parameters s, η, and α. The drive term f in Eq. (2.1) is an arbitrary 2π-periodic function. For $\alpha=1$ and $f=\cos$, we recover the standard definition of the Mathieu equation [25]. For $\alpha\neq 0,1$ we call Eq. (2.1) a *generalized nonlinear Mathieu equation*. It becomes the *nonlinear Mathieu equation* for $\alpha\neq 0,1$ and $f=\cos$. Scaling of the variable x shows that any generalized nonlinear Mathieu equation can be reduced to one of three classes defined by $s=0,\pm 1$.

We start by showing the equivalence of the equations of motion of the single-ion dynamic Kingdon trap with the special case $\alpha=-1$ of the generalized nonlinear Mathieu equation (2.1). The electric field inside a cylinder capacitor is given by

$$E(r,t)=\frac{V(t)}{r\ln(r_2/r_1)}, \tag{2.2}$$

where r_1 and r_2 are the radii of the inner and outer cylinders, respectively, $V(t)$ is the voltage applied to the trap, and r is the distance of the trapped charged particle from the axis of the trap. We define the time average of an arbitrary T-periodic function $h(t)$ by

$$\langle h\rangle=\frac{1}{T}\int_0^T h(t)\,dt. \tag{2.3}$$

The voltage $V(t)$ in Eq. (2.2) is given by

$$V(t)=V_{dc}+V_{ac}g(\omega t). \tag{2.4}$$

It consists of a dc part such that $\langle V(t)\rangle=V_{dc}$ and an ac part of period $T=2\pi/\omega$. The form factor of the ac part is $g(\omega t)$, a 2π-periodic function with zero time average. The radial component of Newton's equation for a particle of mass m and charge Q in the field (2.2) is given by

$$m\ddot{r}=QE(r,t). \tag{2.5}$$

If we define the dimensionless time

$$\tau=\omega t/2 \tag{2.6}$$

and the dimensionless radius

$$x=r\Big/\left[\frac{4|QV_{dc}|}{m\omega^2\ln(r_2/r_1)}\right]^{1/2}, \tag{2.7}$$

Newton's equation (2.5) becomes

$$\ddot{x}+[s-2\eta g(2\tau)]\frac{1}{x}=0, \tag{2.8}$$

where

$$s=\frac{QV_{dc}}{|QV_{dc}|},\quad \eta=-\frac{QV_{ac}}{2|QV_{dc}|}. \tag{2.9}$$

This equation, as claimed in the beginning of this section, is indeed of the form (2.1) with $\alpha=-1$.

We proceed now to show that the equations of motion of a charged particle in a monopole trap are also of the form (2.1). The electric field between the two shells of a spherical capacitor is given by

$$E(r,t)=\frac{r_1r_2}{r_2-r_1}\frac{V(t)}{r^2}, \tag{2.10}$$

where now r_1 and r_2 are the radii of the inner and outer shells, respectively. Introducing the dimensionless time (2.6) and the dimensionless radius

$$x=r\Big/\left[\frac{4|QV_{dc}|}{m\omega^2}\frac{r_1r_2}{r_2-r_1}\right]^{1/3}, \tag{2.11}$$

we obtain from Newton's equation

$$\ddot{x}+[s-2\eta g(2\tau)]\frac{1}{x^2}=0, \tag{2.12}$$

where s and η are defined in Eq. (2.9). This finishes the demonstration of the equivalence of the cylindrical and spherical trap equations with special cases of Eq. (2.1).

III. PSEUDOPOTENTIAL ANALYSIS

The pseudopotential, introduced by Dehmelt [26], is a very useful construct for a qualitative analysis of differential equations with rapidly oscillating drive terms. The pseudopotential is obtained by the method of averaging [27]. In this section we apply the pseudopotential method in order to

search for stable trapping points of the generalized Mathieu equation (2.1).

The pseudopotential $U_{eff}(x)$ for Eq. (2.1) consists of two parts

$$U_{eff}(x)=U_S(x)+U_D(x), \tag{3.1}$$

where $U_S(x)$ originates from the static and $U_D(x)$ from the time-varying components of Eq. (2.1). We have

$$U_S(x)=\begin{cases}\dfrac{s}{\alpha+1}x^{\alpha+1} & \text{for } \alpha\neq -1\\ s\ln|x| & \text{for } \alpha=-1.\end{cases} \tag{3.2}$$

According to Ref. [27], U_D is given by

$$U_D(x)=\frac{\eta^2}{2}\langle f^2\rangle x^{2\alpha}. \tag{3.3}$$

A necessary condition for a trapping point is

$$\frac{dU_{eff}(x)}{dx}=sx^{\alpha}+\alpha\eta^2\langle f^2\rangle x^{2\alpha-1}=0. \tag{3.4}$$

For a minimum we need additionally

$$\frac{d^2U_{eff}(x)}{dx^2}=\alpha s x^{\alpha-1}+\alpha(2\alpha-1)\eta^2\langle f^2\rangle x^{2\alpha-2}>0. \tag{3.5}$$

Several cases have to be considered separately. Although from the mathematical point of view Eq. (2.1) may be investigated for both positive and negative values of x (and in general even for complex x), we restrict ourselves here to the case of $x\geqslant 0$. The only exception are the two integrable cases (ii) and (iv) where both positive and negative x are physical.

(i) $\alpha>1$. According to Eq. (3.4) the location of the extremum is given by

$$x_0=\left[-\frac{s}{\alpha\eta^2\langle f^2\rangle}\right]^{1/(\alpha-1)}. \tag{3.6}$$

Apparently, a physical extremum exists only for $s=-1$. According to Eq. (3.5), it is always a minimum. The case (i) is relevant for higher multipole traps [28].

(ii) $\alpha=1$. This is the integrable case of the ordinary Mathieu equation. It corresponds to the Paul trap [5]. According to Eqs. (3.4) and (3.5), the discussion of the existence and stability of trapping points depends on the value of the parameter

$$p=s+\eta^2\langle f^2\rangle. \tag{3.7}$$

Since the pseudopotential analysis is valid only for small η, we can rule out the case $p=0$. Thus Eq. (3.4) has a single solution $x=0$. According to Eq. (3.5), it is a minimum for $p>0$. Since η is small this requires $s=1$.

(iii) $0<\alpha<1$. The extremum is again given by Eq. (3.6). However, for case (iii) it does not correspond to a minimum.

(iv) $\alpha=0$. This is another integrable case of the generalized Mathieu equation (2.1).

(v) $\alpha<0$. The extremum is given by Eq. (3.6), but this time $s=1$. All the extrema are minima. Special cases of (v) are the dynamic Kingdon trap and the monopole trap. We specialize now to $f=\cos$ and $\alpha=-1$. This case corresponds to the dynamic Kingdon trap. We obtain $x_0=|\eta|/\sqrt{2}$, recovering the equilibrium solution computed in Ref. [15]. The case $f=\cos$ and $\alpha=-2$ corresponds to the monopole trap. We obtain $x_0=|\eta|^{2/3}$. This is the dimensionless version of the equilibrium point computed in Ref. [22].

This finishes our qualitative discussion of equilibrium points of Eq. (2.1) in the pseudo-potential approximation. In the following section we keep the time dependence and investigate numerically and analytically the exact behavior of Eq. (2.1).

IV. BIFURCATION SCENARIO AND CHAOS OF CW-DRIVEN TRAPS

According to the pseudopotential analysis presented in Sec. III, the dynamic Kingdon trap exhibits a pseudopotential minimum for all $\eta>0$. This minimum, however, does not always correspond to simple motion of the trapped ion. As a function of decreasing η, the ion undergoes bifurcations and eventually exhibits a chaos transition at some critical value η^*. In order to illustrate the bifurcation scenario of the cw-driven dynamic Kingdon trap we solved the damped dynamic Kingdon equation

$$\ddot{x}+\gamma\dot{x}+[1-2\eta\cos(2\tau)]\frac{1}{x}=0 \tag{4.1}$$

for $\gamma=0.01$ while slowly decreasing the control parameter η. We obtain the bifurcation diagram shown in Fig. 1(a) with bifurcations at $\eta_1\approx 3.12$ and $\eta_2\approx 2.94$. The diagram shows the position of the ion $x_n=x(n\pi)$ (n is an integer) as a function of η. For $\eta>\eta_1$ the motion converges to a simple π-periodic limit cycle. This is the range of control parameters where the pseudopotential analysis is valid. There is an accumulation of bifurcations for $\eta^*\approx 2.91$ [not shown in Fig. 1(a)].

We now want to obtain some analytical insight into the location of the first bifurcation point at η_1. The following analytical derivations are based on the dynamic Kingdon equation (4.1) for $\gamma=0$. For $\eta>\eta_1$ the limit cycle of Eq. (4.1) is π periodic. Therefore, we expand the solution in this region according to

$$x=\sum_{\nu=0}^{\infty}A_\nu\cos(2\nu\tau). \tag{4.2}$$

Substituting Eq. (4.2) into Eq. (4.1), we obtain

$$2\sum_{\nu,\mu=0}^{\infty}A_\nu A_\mu\mu^2\{\cos[2\tau(\nu+\mu)]+\cos[2\tau(\nu-\mu)]\}+2\eta\cos(2\tau)-1=0. \tag{4.3}$$

Keeping only the first two terms in Eq. (4.2), we obtain

$$A_0=\pm\eta/\sqrt{2},\quad A_1=\mp 1/\sqrt{2}, \tag{4.4}$$

hence

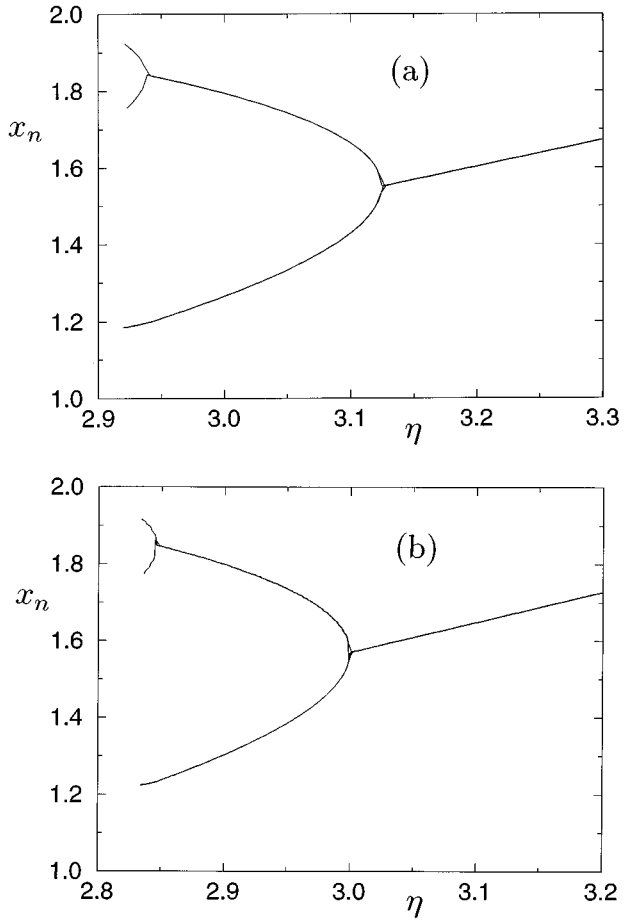

FIG. 1. Bifurcation diagram of the dynamic Kingdon trap. Plotted is the scaled position of a charged particle in the trap at times $\tau = n\pi$ (n is an integer) as a function of the control parameter η. (a) The cw-driven dynamic Kingdon trap and (b) the kicked Kingdon trap.

$$x \approx [\eta - \cos(2\tau)]/\sqrt{2}. \tag{4.5}$$

At the first bifurcation the period of the limit cycle doubles. Thus, for $\eta < \eta_1$ we consider the solution

$$x = \sum_{\nu=0}^{\infty} B_\nu \cos(\nu\tau). \tag{4.6}$$

In this case keeping the first three terms in Eq. (4.6), we obtain two solutions. The first one, $B_0 = A_0$, $B_1 = 0$, and $B_2 = A_1$, is identical to Eq. (4.5). A second nontrivial solution is given by

$$B_0 = \frac{5}{24}\sqrt{12(2\eta+1)}, \quad B_1 = \sqrt{(5-2\eta)/3},$$

$$B_2 = -\sqrt{(2\eta+1)/12}. \tag{4.7}$$

At $\eta = \eta_1$ Eqs. (4.2) and (4.6) must be the same. This implies $B_1(\eta_1) = 0$ and thus $\eta_1 = 5/2$.

A better approximation of η_1 is obtained by keeping one more term in Eq. (4.6). We obtain the four conditions

$$B_1^2 + 4B_2^2 + 9B_3^2 - 2 = 0, \tag{4.8a}$$

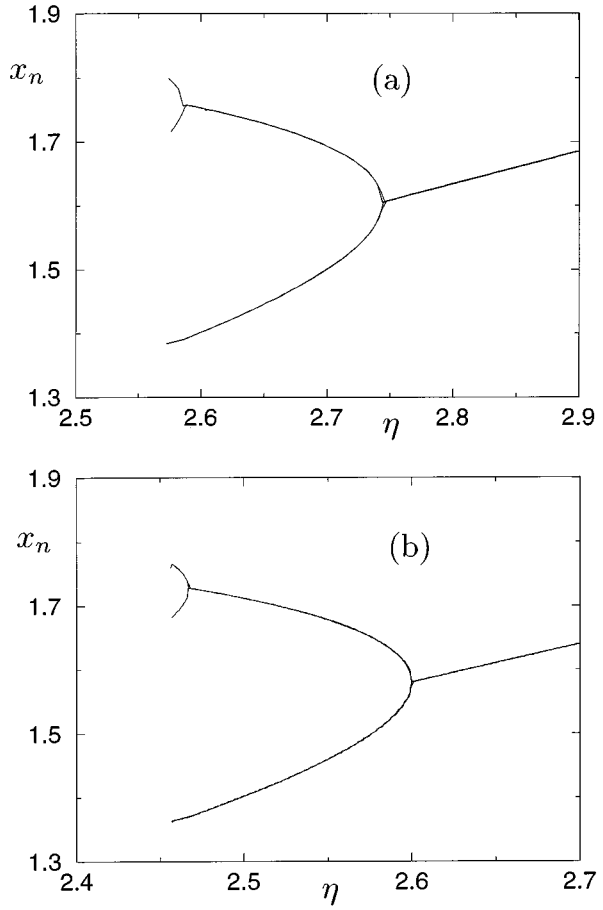

FIG. 2. Same as Fig. 1, but for the monopole trap.

$$2B_0B_1 + 5B_1B_2 + 13B_2B_3 = 0, \tag{4.8b}$$

$$8B_0B_2 + B_1^2 + 10B_1B_3 + 4\eta = 0, \tag{4.8c}$$

$$18B_0B_3 + 5B_1B_2 = 0. \tag{4.8d}$$

Close to the first bifurcation we have $B_0 \to \pm\eta/\sqrt{2}$, $B_1 \to 0$, $B_2 \to \mp 1/\sqrt{2}$, and $B_3 \to 0$. From Eqs. (4.8b) and (4.8d) we obtain

$$36B_0^2 + 90B_0B_2 - 65B_2^2 = 0. \tag{4.9}$$

Using the limiting values for B_0 and B_2 in Eq. (4.9) we obtain

$$\eta_1 = \frac{15 + \sqrt{485}}{12} \approx 3.085. \tag{4.10}$$

The relative error of this result is of the order of 1%.

We show now that the bifurcation diagram of the monopole trap ($\alpha = -2$) is qualitatively the same as the bifurcation diagram for the dynamic Kingdon equation. Solving numerically the monopole equation

$$\ddot{x} + \gamma\dot{x} + [1 - 2\eta\cos(2\tau)]\frac{1}{x^2} = 0, \tag{4.11}$$

we obtain the bifurcation diagram shown in Fig. 2(a). Thus both the dynamic Kingdon trap and the monopole trap ex-

hibit a period-doubling cascade into chaos. An analytical estimate of η_1 for the monopole trap along the lines of Eqs. (4.2)–(4.7) yields $\eta_1=(35+5\sqrt{7})/24\approx 2$. In analogy to the dynamic Kingdon trap, this result can be improved by keeping more terms in the Fourier expansions of x.

Both the dynamic Kingdon trap and the monopole trap are nonlinear Hamiltonian systems. Such systems generically exhibit a mixed phase space at any value of the system parameters. Thus we suspect that even for $\eta>\eta_1$ both traps exhibit Hamiltonian chaos in some parts of their phase space. This is confirmed in Fig. 3(a), where we show a Poincaré surface of section for the dynamic Kingdon trap for $\eta=4$. We see a large elliptic island surrounded by intricate island chains and chaos. The elliptic island in Fig. 3(a) corresponds to the stable trapping region of the dynamic Kingdon trap.

In Fig. 3(b) we show a phase-space portrait for $\eta=3.05$, i.e., after the first bifurcation of Fig. 1(a). The stable island of Fig. 3(a) has split into two stable islands with surrounding chaos. The two islands of Fig. 3(b) split into four islands after the second bifurcation at $\eta=\eta_2$. This situation is shown in Fig. 3(c). The two islands of Fig. 3(b) have split into four islands located at $x\approx 1.2$ and $x\approx 1.8$. The two islands at $x\approx 1.2$, however, are not resolved on the scale of Fig. 3(c).

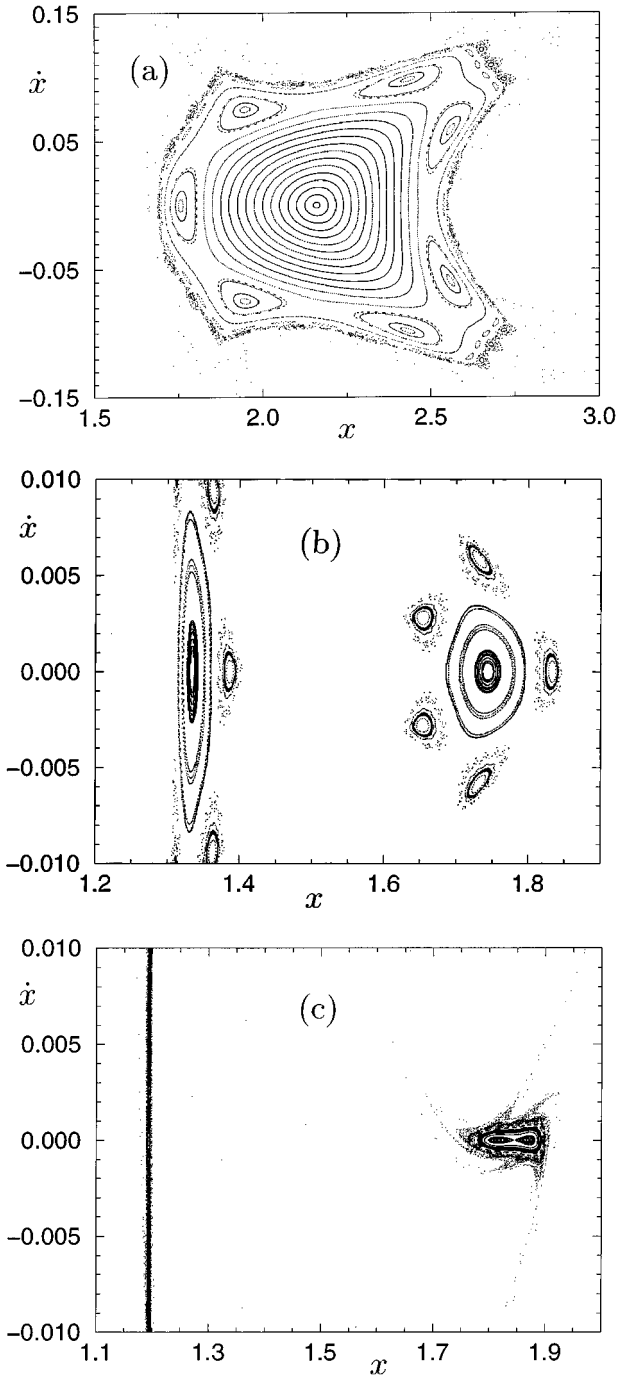

FIG. 3. Poincaré sections for the dynamic Kingdon trap at different values of the control parameter η: (a) $\eta=4$ (before the first bifurcation), (b) $\eta=3.05$ (after the first bifurcation), and (c) $\eta=2.936$ (after the second bifurcation).

V. KICKED TRAPS

In this section we present a detailed analysis of a class of generalized nonlinear Mathieu equations where the drive term f is a train of alternating δ kicks. The strength and frequency of the δ kicks are adjusted such that the fundamental harmonic of the array of δ kicks coincides with the drive term $2\eta\cos(2\tau)$ of a cw-driven trap. Inasmuch as higher harmonics do not contribute appreciably to the dynamics of the particle, the cw-driven problem can be replaced by the kicked problem, a problem much more amenable to analytical treatment. In fact, we will show that the bifurcation scenarios for the cw-driven problem and the kicked problem are qualitatively identical and quantitatively very close to each other. Thus, replacing the cw drive with a train of δ kicks offers substantial insight into the mechanism of the bifurcation cascades that occur in these traps.

In what follows we assume without loss of generality $\eta\geqslant 0$. The case $\eta<0$ can be recovered trivially by a shift of τ. Only for $s=1$ is stable trapping possible. For all the classic traps (static Kingdon, Paul, and Penning) the equations of motion of a single charged particle are integrable. This is the reason for the absence of single-ion chaos in the ideal versions of these traps. The Kingdon equation (4.1), however, is nonlinear, a necessary ingredient for chaos. That the nonlinearity exhibited by Eq. (4.1) is also sufficient for Eq. (4.1) to possess chaotic solutions has already been shown in Sec. IV (see Fig. 3). Insight and analytical control over the route to chaos can be derived from the kicked Kingdon trap.

The starting point is the nonlinear Mathieu equation

$$\ddot{x}+[s-2\eta\cos(2\tau)]x^{\alpha}=0. \tag{5.1}$$

The aim is to represent the drive term $s-2\eta\cos(2\tau)$ in Eq. (5.1) as accurately as possible with the help of π-periodic δ functions $\delta_\pi(\tau)$. One possibility is to replace the drive term with $a+b\,\delta_\pi(\tau)$, where a and b are constants to be adjusted for best results. In this case, however, the constant a forces us to solve the one-dimensional equations of motion of the ion in a $1/x$ potential. Although trivially integrable, the presence of the static $1/x$ potential considerably complicates the resulting mapping equations. This problem is avoided by modeling the drive term in the square brackets in Eq. (5.1) by a train of alternating δ kicks. This way we obtain the equation of motion

$$\ddot{x}+[-a\,\delta_\pi(\tau)+b\,\delta_\pi(\tau-\pi/2)]x^{\alpha}=0, \tag{5.2}$$

where $\delta_\pi(\tau)$ is the π-periodic δ function. Its Fourier expansion is

$$\delta_\pi(\tau)=\frac{1}{\pi}\sum_{\nu=-\infty}^{\infty}\exp(2i\nu\tau). \tag{5.3}$$

Using Eq. (5.3) we have

$$\begin{aligned}&[-a\,\delta_\pi(\tau)+b\,\delta_\pi(\tau-\pi/2)]\\&\quad=-\frac{1}{\pi}[(a-b)+2(a+b)\cos(2\tau)\\&\qquad+2(a-b)\cos(4\tau)+\cdots].\end{aligned} \tag{5.4}$$

Thus, neglecting higher harmonics in Eq. (5.4), a good approximation to Eq. (5.1) is obtained if we choose

$$a=\frac{\pi}{2}(\eta-s),\quad b=\frac{\pi}{2}(\eta+s). \tag{5.5}$$

We denote by (x_n,v_n) the values of x and $\dot{x}$ immediately before the kick at $\tau=n\pi$ and by (x_n',v_n') the respective values immediately after the kick at $\tau=n\pi$. Also, we denote by $(\tilde{x}_n,\tilde{v}_n)$ the values of x and $\dot{x}$ immediately before the kick at $\tau=(n+1/2)\pi$ and by $(\tilde{x}_n',\tilde{v}_n')$ the respective values immediately after the kick at $\tau=(n+1/2)\pi$. Then the solution of Eq. (5.2) is obtained analytically as a mapping from kick number n to kick number $n+1$ composed of four steps. (i) propagation over the kick at $\tau=n\pi$,

$$x_n'=x_n,\quad v_n'=v_n+ax_n^\alpha; \tag{5.6}$$

(ii) free propagation to the kick at $\tau=(n+1/2)\pi$,

$$\tilde{x}_n=x_n+\pi v_n'/2,\quad \tilde{v}_n=v_n'; \tag{5.7}$$

(iii) propagation over the kick at $\tau=(n+1/2)\pi$,

$$\tilde{x}_n'=\tilde{x}_n,\quad \tilde{v}_n'=\tilde{v}_n-b\tilde{x}_n^\alpha; \tag{5.8}$$

and (iv) free propagation to the kick at $\tau=(n+1)\pi$,

$$x_{n+1}=\tilde{x}_n'+\pi\tilde{v}_n'/2,\quad v_{n+1}=\tilde{v}_n'. \tag{5.9}$$

The four steps (5.6)–(5.9) can be condensed into one. We obtain a mapping that propagates from the kick at $\tau=n\pi$ to the kick at $\tau=(n+1)\pi$:

$$\begin{aligned}x_{n+1}&=x_n+\pi(v_n+ax_n^\alpha)-\frac{\pi}{2}b\left[x_n+\frac{\pi}{2}(v_n+ax_n^\alpha)\right]^\alpha,\\v_{n+1}&=v_n+ax_n^\alpha-b\left[x_n+\frac{\pi}{2}(v_n+ax_n^\alpha)\right]^\alpha.\end{aligned} \tag{5.10}$$

The fixed point of Eq. (5.10) is given by

$$x^{(1)}=\left\{\frac{4}{a\pi}[(a/b)^{1/\alpha}-1]\right\}^{1/(\alpha-1)},\quad v^{(1)}=-\frac{a}{2}[x^{(1)}]^\alpha. \tag{5.11}$$

Physically the fixed point is important because it corresponds to the stable minimum in which the trapped particle settles in the presence of cooling. The first bifurcation happens at the value η_1 where the fixed point turns unstable. The stability properties of the fixed point are determined by the Jacobian matrix

$$J=\begin{pmatrix}\dfrac{\partial x_{n+1}}{\partial x_n} & \dfrac{\partial x_{n+1}}{\partial v_n}\\[2ex]\dfrac{\partial v_{n+1}}{\partial x_n} & \dfrac{\partial v_{n+1}}{\partial v_n}\end{pmatrix} \tag{5.12}$$

evaluated at the fixed point. Since the mapping (5.10) represents a Hamiltonian flow, the determinant of the Jacobian matrix J has absolute magnitude 1. Thus the stability of the fixed point is determined by the trace of J. For $|\mathrm{Tr}(J)|<2$ the eigenvalues of J are complex conjugate points on the unit circle. Thus, the fixed point is stable for $|\mathrm{Tr}(J)|<2$. For $|\mathrm{Tr}(J)|>2$ exactly one of the eigenvalues of J exceeds 1 in absolute magnitude and the fixed point is unstable. Thus the first bifurcation happens exactly at $|\mathrm{Tr}(J)|=2$. The trace of J is easily evaluated. At the fixed point we obtain

$$\mathrm{Tr}(J)=2+4\alpha(\alpha-1)(\rho-1)\left(\frac{1}{\rho}-1\right), \tag{5.13}$$

where

$$\rho=\left(\frac{\eta-s}{\eta+s}\right)^{1/\alpha}. \tag{5.14}$$

For $\rho>0$ we have $\mathrm{Tr}(J)<2$. Thus the first bifurcation happens at $\mathrm{Tr}(J)=-2$, which yields

$$\rho_1=1+\frac{1}{\alpha}\{1\pm\sqrt{4\alpha(\alpha-1)+1}\} \tag{5.15}$$

or

$$\eta_1=s\frac{1+\rho_1^\alpha}{1-\rho_1^\alpha}. \tag{5.16}$$

Specializing to $\alpha=-1$ (the dynamic Kingdon trap), we obtain the mapping

$$\begin{aligned}x_{n+1}&=x_n+\pi(v_n+a/x_n)-\frac{\pi}{2}bx_n/(x_n^2+\pi x_nv_n/2+\pi a/2),\\v_{n+1}&=v_n+a/x_n-bx_n/(x_n^2+\pi x_nv_n/2+\pi a/2).\end{aligned} \tag{5.17}$$

From Eq. (5.11) we obtain the fixed point and the velocity at the fixed point

$$x^{(1)}=\frac{\pi}{4}\,|\eta-1|, \quad v^{(1)}=-\mathrm{sgn}(\eta-1). \tag{5.18}$$

Approaching $\eta=1$ from large values of η, Eq. (5.18) tells us that the radial position of the trapped particle approaches monotonically the location of the inner electrode. Since $x^{(1)}=0$ for $\eta=1$ this means that the particle encounters the inner electrode at some $\eta_c>1$. Thus we obtain a lower bound $\eta>\eta_c>1$ for physically meaningful η values.

For $\alpha=-1$ the trace of the Jacobian is given by

$$\mathrm{Tr}(J)=2-32/(\eta^2-1). \tag{5.19}$$

We see that for large η, $|\mathrm{Tr}(J)|<2$, i.e., the fixed point is stable and so is the trap. In practical terms the result (5.19) means that there is no problem with finding a suitable operation point for the dynamic Kingdon trap since any η will lead to stable trapping if only η is sufficiently large. According to Eq. (5.16), the first bifurcation happens at $\eta_1=3$. This result is very close to the position of the first bifurcation of the continuously driven dynamic Kingdon trap that was determined to occur at $\eta_1=3.124\ldots$ [15].

It is even possible to compute the location of the second bifurcation of the mapping (5.17) analytically. The computations are lengthy and tedious and are not reproduced here. The result is $\eta_2=37/13=2.846\ldots$. This result too compares very favorably with the location of the second bifurcation of the cw-driven dynamic Kingdon trap computed to be $\eta_2=2.938\ldots$ [15].

Specializing to $\alpha=-2$ (the monopole trap), we obtain $\rho_1=3$. From ρ_1 we compute $\eta_1=5/4$ and $x^{(1)}=\pi/16$. Again these results compare favorably with the location of the fixed point and the location of the first bifurcation of the monopole trap.

Laser cooling is simulated by adding a small damping term to Eq. (5.2). We obtain the damped kicked nonlinear Mathieu equation

$$\ddot{x}+\gamma\dot{x}+[-a\,\delta_\pi(\tau)+b\,\delta_\pi(\tau-\pi/2)]x^\alpha=0. \tag{5.20}$$

In analogy to Eq. (5.10) we obtain the mapping equations for Eq. (5.20) in the form

$$x_{n+1}=x_n+\mu(1+\lambda)(v_n+ax_n^\alpha)-b\mu[x_n+\mu(v_n+ax_n^\alpha)]^\alpha, \tag{5.21}$$

$$v_{n+1}=\lambda^2(v_n+ax_n^\alpha)-b\lambda[x_n+\mu(v_n+ax_n^\alpha)]^\alpha,$$

where

$$\lambda=\exp(-\gamma\pi/2), \quad \mu=(1-\lambda)/\gamma. \tag{5.22}$$

The damping term ensures that we follow adiabatically the stable branches of the bifurcation tree. With $\gamma=0.01$ we obtain the bifurcation diagram shown in Fig. 1(b). It may be compared with the bifurcation diagram of the continuously driven dynamic Kingdon trap shown in Fig. 1(a). The bifurcation diagrams are qualitatively the same and quantitatively similar. This proves that even as far as the route to chaos is concerned, the kicked Kingdon trap is a very good model for the cw-driven dynamic Kingdon trap. It should also be mentioned that kicked traps not only are a useful construct in our analysis of the cw-driven traps but they are also a theoretically legitimate and practically realizable model in themselves.

VI. DISCUSSION

It may seem that the dynamic Kingdon trap is not a realistic device since it requires the cylinder to be infinitely extended. This is not the case. A finite device is obtained either by the use of end caps [15] or by ''tapering'' the ends of the cylinder. This way the trapped particle is focused towards the symmetry plane of the trap, where it experiences exactly the same forces as in the case of an infinite cylinder. Thus all the theoretical analysis presented in the previous sections applies without change to tapered traps or traps with end caps. That this principle works in practice was recently demonstrated with the open geometry monopole trap [22].

Another cause for concern may be the use of impulsive kicks in our analytical analysis presented in Sec. V. It is true that in the case of cw-driven traps the kicks are an approximation to the continuous time dependence of the drive term. This approximation becomes progressively better as the drive term is approximated with more and more kicks. However, there is another way of looking at the kicks. The kicks may become an excellent approximation to the exact time dependence of the drive term in case the traps are driven with narrow pulses generated by a pulse generator. Such schemes were previously suggested in the context of localization studies with diatomic molecules [29]. However, while the driven molecules need to be perturbed with pulses with a repetition rate of the order of gigahertz, and require a pulse width of the order of picoseconds, the pulses for the realization of a kicked Kingdon trap, e.g., may be in the megahertz region where sharp pulses can be produced without any technical problems. The frequency requirements are even less stringent in the case of trapped macroscopic particles [22,30].

VII. SUMMARY AND CONCLUSIONS

In this paper we presented a detailed analysis of the dynamic Kingdon trap and the monopole trap for cw and impulsive drives. In the course of our analysis it proved convenient to define a class of nonlinear equations, the generalized nonlinear Mathieu equations. These equations themselves constitute a promising field of analysis for future investigations. We presented a qualitative analysis of the generalized nonlinear Mathieu equations within the framework of the pseudopotential theory. We showed that both traps, the dynamic Kingdon trap and the monopole trap, exhibit a bifurcation scenario of the fundamental stable trapping island. In addition we showed in the case of the dynamic Kingdon trap that the trapping island is surrounded by Hamiltonian chaos. We succeeded in computing analytically the location of the first bifurcation for the kicked nonlinear Mathieu equations. In the case of the kicked dynamic Kingdon equation we were able to compute analytically the location of the second bifurcation point. Approximate analytical expressions for the location of the first bifurcation point were computed in the case of the cw-driven traps. Experiments, such as the one

conducted at the Max-Planck-Institute in Munich, are now beginning to explore the rich dynamics of this class of traps. Of special interest is the quantum mechanics at bifurcation points. We propose to use strongly defocusing traps such as the dynamic Kingdon trap or the monopole trap as experimental devices for the exploration of this topic of basic quantum-mechanics research.

ACKNOWLEDGMENTS

We thank E. Teloy for bringing early unpublished research on the dynamic Kingdon trap conducted at Freiburg University to our attention. Financial support by the Deutsche Forschungsgemeinschaft (Grant No. SFB 276) is gratefully acknowledged.

[1] K. H. Kingdon, Phys. Rev. **21**, 408 (1923).
[2] D. A. Church, Phys. Scr. **T59**, 216 (1995).
[3] F. M. Penning, Physica (Amsterdam) **3**, 873 (1936).
[4] H. Dehmelt, Rev. Mod. Phys. **62**, 525 (1990).
[5] W. Paul, W. Osberghaus, and E. Fischer, Forsch. Wirtsch. Verkehrsminist. Nordrhein Westfalen **415**, 1 (1958).
[6] W. Paul, Rev. Mod. Phys. **62**, 531 (1990).
[7] H. Dehmelt, Phys. Scr. **T59**, 303 (1995).
[8] R. Blümel, C. Kappler, W. Quint, and H. Walther, Phys. Rev. A **40**, 808 (1989).
[9] J. Hoffnagle and R. G. Brewer, Phys. Rev. A **50**, 4157 (1994).
[10] J. J. Bollinger, D. J. Heinzen, W. M. Itano, S. L. Gilbert, and D. J. Wineland, IEEE Trans. Instrum. Meas. **40**, 126 (1991).
[11] J. I. Cirac and P. Zoller, Phys. Rev. Lett. **74**, 4091 (1995).
[12] H. Straubel, Naturwissenschaften **42**, 506 (1955).
[13] C. A. Schrama, E. Peik, W. W. Smith, and H. Walther, Opt. Commun. **101**, 32 (1993).
[14] R. G. Lerner and G. L. Trigg, *Encyclopedia of Physics*, 2nd ed. (VCH, New York, 1991), p. 1239.
[15] R. Blümel, Phys. Rev. A **51**, R30 (1995).
[16] R. Blümel, Appl. Phys. B: Lasers Opt. **60**, 119 (1995).
[17] R. Blümel, Phys. Scr. **T59**, 369 (1995).
[18] E. Teloy (private communication).
[19] R. E. Bahr, Diplomarbeit, Physikalisches Institut der Universität Freiburg, 1969 (unpublished).
[20] E. Behre, Zulassungsarbeit, Physikalisches Institut der Universität Freiburg, 1972 (unpublished).
[21] T. W. Hänsch and A. L. Schawlow, Opt. Commun. **13**, 68 (1975).
[22] E. Peik and J. Fletcher (unpublished).
[23] S. Stenholm, Rev. Mod. Phys. **58**, 699 (1986).
[24] D. J. Wineland and W. M. Itano, Phys. Today **40**(6), 34 (1987).
[25] *Handbook of Mathematical Functions*, Appl. Math. Ser. No. 55, edited by M. Abramowitz and I. A. Stegun (U.S. GPO, Washington, DC, Natl. Bur. Stand. 1964).
[26] H. G. Dehmelt, Adv. At. Mol. Phys. **3**, 53 (1967).
[27] L. D. Landau and E. M. Lifshitz, *Mechanics* (Pergamon, Oxford, 1960).
[28] J. Walz, I. Siemers, M. Schubert, W. Neuhauser, and R. Blatt, Europhys. Lett. **21**, 183 (1993).
[29] R. Blümel, S. Fishman, and U. Smilansky, J. Chem. Phys. **84**, 2604 (1986).
[30] J. Hoffnagle and R. G. Brewer, Phys. Rev. Lett. **71**, 1828 (1993).